Published in "The Journal of Comparative Neurology 502(5): 834 - 847, 2007"
which should be cited to refer to this work.

Architecture of the Primary Taste Center of *Drosophila melanogaster* Larvae

JULIEN COLOMB,* NICOLA GRILLENZONI, ARIANE RAMAEKERS, AND REINHARD F. STOCKER
Department of Biology and Program in Neuroscience, University of Fribourg, 1700 Fribourg, Switzerland

http://doc.rero.ch

ABSTRACT

A simple nervous system combined with stereotypic behavioral responses to tastants, together with powerful genetic and molecular tools, have turned *Drosophila* larvae into a very promising model for studying gustatory coding. Using the Gal4/UAS system and confocal microscopy for visualizing gustatory afferents, we provide a description of the primary taste center in the larval central nervous system. Essentially, gustatory receptor neurons target different areas of the subesophageal ganglion (SOG), depending on their segmental and sensory organ origin. We define two major and two smaller subregions in the SOG. One of the major areas is a target of pharyngeal sensilla, the other one receives inputs from both internal and external sensilla. In addition to such spatial organization of the taste center, circumstantial evidence suggests a subtle functional organization: aversive and attractive stimuli might be processed in the anterior and posterior part of the SOG, respectively. Our results also suggest less coexpression of gustatory receptors than proposed in prior studies. Finally, projections of putative second-order taste neurons seem to cover large areas of the SOG. These neurons may thus receive multiple gustatory inputs. This suggests broad sensitivity of secondary taste neurons, reminiscent of the situation in mammals.

The primary goal of chemosensory neurobiology is to understand how information about the chemical environment is encoded by the nervous system. *Drosophila* is being intensely used as a model system for deciphering the olfactory code (Keller and Vosshall, 2003; Dahanukar et al., 2005; Jefferis, 2005; Rutzler and Zwiebel, 2005; Hallem et al., 2006). The recent discovery of a family of gustatory receptors (GRs) in the fly (Clyne et al., 2000; Scott et al., 2001) has also boosted interest in the study of taste. The simple nervous system of *Drosophila* larvae, in combination with powerful genetic and molecular tools, may be of great advantage for studying gustatory coding principles. Moreover, larvae exhibit interesting behaviors in response to tastants. They can discriminate between different salts and different sugars (Miyakawa, 1982) and are able to use gustatory information as reward (Scherer et al., 2003; Gerber et al., 2004).

While olfactory coding in adult *Drosophila* relies on a multitude of combinatorial patterns of activity in olfactory glomeruli (Keller and Vosshall, 2003), taste information appears to be assigned to a small number of categories in the periphery (Scott, 2004). In mammals, mutually exclusive groups of gustatory receptor cells appear to respond to sweet and bitter taste ("labeled line" coding; Zhao et al., 2003; Mueller et al., 2005), although electrophysiological and molecular data contradict each other to some extent (reviewed in Meyerhof, 2005). For instance, whether finer discrimination within a category occurs in the periphery is currently in debate (Caicedo and Roper, 2001; see also Glendinning et al., 2002). In contrast, central neuronal

Grant sponsor: Swiss National Funds; Grant numbers: 31-63447.00, 3100A0-105517 (to R.F.S.) and 3234-069273.02 (to A.R.).

*Correspondence to: Dr. Julien Colomb, Gènes et Dynamique des Systèmes de Mémoire, CNRS UMR 7637, ESPCI 10, rue Vauquelin, F-75005 Paris, France. E-mail: Julien.colomb@espci.fr

http://doc.rero.ch

responses become broadly tuned to multiple categories (Sato and Beidler, 1997; Lemon and Smith, 2005). These data suggest that taste information in the brain depends on the pattern of activity across neurons ("across-fiber" coding) (Smith and St John, 1999; Lemon and Smith, 2006; Stapleton et al., 2006). However, a recent review proposed that both models are too static to account for the high modulation of gustatory responses (Jones et al., 2006).

In *Drosophila* and other insects, adult taste sensilla usually contain four gustatory receptor neurons (GRNs), which were shown to respond to either water, sugar, or low or high salt concentrations (Ishimoto and Tanimura, 2004). Deterrent compounds (sensed as bitter by humans) appear to activate a subset of salt-responding cells. Interestingly, despite their generally broad tuning (Marella et al., 2006), at least some of the bitter-responding GRNs exhibit a certain degree of selectivity (Meunier et al., 2003). Flies should thus be able to discriminate between certain bitter compounds. Sweet and deterrent compounds seem to be recognized by a family of seven transmembrane GRs, which are related to odorant receptors (reviewed in Scott et al., 2001; Robertson et al., 2003; Hallem et al., 2006). For instance, GR5a was shown to be the receptor responsive for trehalose perception (Dahanukar et al., 2001; Ueno et al., 2001; Inomata et al., 2004) and GR66a was proposed to be a caffeine receptor (Moon et al., 2006). More surprising, GR21a is expressed in CO_2-responsive olfactory cells in the antenna (Suh et al., 2004) and was recently suggested to be expressed in CO_2-responsive cells in larvae as well (Faucher et al., 2006). In contrast, salt responses are not mediated by GRs, but by ionic channels encoded by the *pickpocket* gene family (ppk) (Liu et al., 2003a). Finally, proteins of the transient receptor potential (TRP) family were also shown to be involved in chemical perception (Al-Anzi et al., 2006), perhaps indirectly, apart from their role in pain and temperature sensation (Tracey et al., 2003).

The expression pattern of the GR genes in adults was essentially assessed indirectly, via Gal4 reporter gene expression (Dunipace et al., 2001; Scott et al., 2001; Liu et al., 2003a; Thorne et al., 2004; Wang et al., 2004; Marella et al., 2006). Although reporter expression patterns may not accurately reflect GR expression patterns, the collected data suggest that many GRNs coexpress multiple receptors. For instance, the majority of GRs seem to be expressed in Gr66a-expressing cells, which mediate aversive behavior (Thorne et al., 2004; Wang et al., 2004). Moreover, the majority of sugar-responsive cells appear to coexpress at least three different, but molecularly uncharacterized, sugar receptive sites (Ishimoto and Tanimura, 2004). However, as a principle, putative sugar GRs and bitter GRs seem to be expressed in different subsets of GRNs. This allows initiation of distinct behavioral responses, i.e., attraction versus repulsion (Marella et al., 2006), similar to mammals (Zhao et al., 2003; Mueller et al., 2005). In insects, few data on central gustatory processing have been collected (Mitchell et al., 1999).

The central projection patterns of adult GRNs established by reporter gene expression (Thorne et al., 2004; Wang et al., 2004) correlate well with previous reports (Stocker and Schorderet, 1981; Nayak and Singh, 1985; Shanbhag and Singh, 1992). First, projections from different gustatory organs segregate in the subesophageal ganglion (SOG). Second, central projections of GRNs sensitive to attractive and aversive cues are distinct (Thorne et al., 2004; Wang et al., 2004; Marella et al., 2006). Third, labellar GRNs mediating aversive behavior project bilaterally, whereas those responsible for attractive behavior remain ipsilateral (Thorne et al., 2004; Wang et al., 2004). Bilateral projections are also typical for pharyngeal sensilla (Stocker and Schorderet, 1981; Rajashekhar and Singh, 1994).

The larval taste system is less well documented. It also comprises external and internal sense organs, most of which are multimodal (Stocker, 1994). External organs include the terminal organ (TO; with taste, stretch, touch, and thermoreceptive neurons), the ventral organ (VO; with taste and touch receptors), and the dorsal organ (DO) (Singh and Singh, 1984; Stocker, 1994; Python and Stocker, 2002). The DO is the unique larval olfactory organ (Fishilevich et al., 2005), which in addition contains putative mechanoreceptive and taste sensilla (Stocker, 1994). Other putative taste organs may occur in thoracic and abdominal segments (Dambly-Chaudière and Ghysen, 1986). Gustatory identity is suggested from the presence of polyinnervation and their dependence on the taste sensillum-specific *poxn* gene (Dambly-Chaudière et al., 1992). Internal chemosensory organs comprise the dorsal, ventral, and posterior pharyngeal sense organs (DPS, VPS, and PPS, respectively) and the dorsal pharyngeal organ (DPO) (Gendre et al., 2004). The axons deriving from the DO as well as three axons from the TO project to the brain via the antennal nerve, while the other TO neurons and all of the VO neurons pass to the SOG through the maxillary nerve. Fibers from the DPS, DPO, and PPS travel via the labral nerve, while those from VPS follow the labial nerve (Fig. 1) (Python and Stocker, 2002).

Electrophysiological recording of the TO demonstrates taste (Oppliger et al., 2000) and thermosensory function (Liu et al., 2003b). In addition, when the cells labeled by the enhancer trap line GH86 were inactivated or ablated, thermotaxis (Liu et al., 2003b) and chemotaxis toward fructose and salt (Heimbeck et al., 1999) were affected. Since this line shows the strongest expression in the TO (and only minor expression in other peripheral neurons or nonneuronal cells), the behavioral deficit was suggested to be due to the inactivation of TO neurons (Heimbeck et al., 1999).

Abbreviations

AN	Antennal nerve
ChAT	Choline acetyl-transferase
DO	Dorsal organ
DPO	Dorsal pharyngeal organ
DPS	Dorsal pharyngeal sense organ
GR	Gustatory receptor protein
LbN	Labial nerve
LrN	Labral nerve
MN	Maxillary nerve
Ppk	Pickpocket (gene family)
PPS	Posterior pharyngeal sense organ
SOG	Subesophageal ganglion
TO	Terminal organ
TODO	3 special neurons belonging to the TO but going via the antennal nerve
VO	Ventral organ
VPS	Ventral pharyngeal sense organ

http://doc.rero.ch

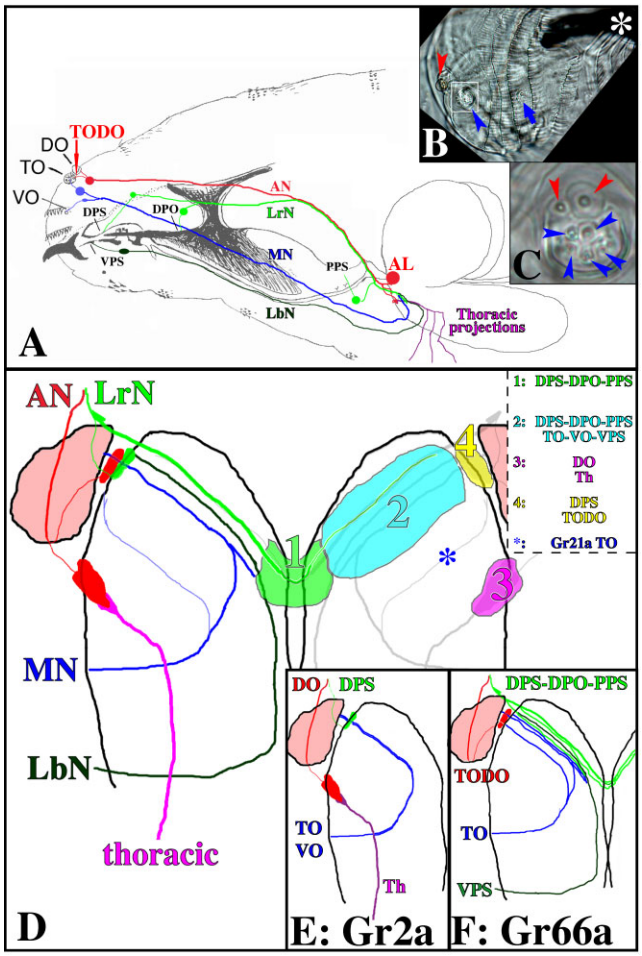

Fig. 1. Diagrams of larval head chemosensory organs (**A–C**), their nerves (A) and their central target areas (**D–F,** horizontal views). Black lines in D–F represent the neuropile borders established by anti-ChAT labeling (cf. Fig. 2); the antennal lobe is show in light red. A: The different peripheral nerves and the origin of the afferents that they carry are shown in different colors. Note an atypical DO neuron whose dendrites extend in the TO (TODO). The entry points of the nerves in the SOG were deduced from confocal images at horizontal orientation. B: Ventral view (Nomarski optics) of the DO with its prominent olfactory "dome" (red arrowhead), the TO (blue arrowhead), the VO (blue arrow), and the mouth hooks (asterisk). C: Close-up of TO showing two "dorsolateral" sensilla (red arrowheads) and five "distal" sensilla (blue arrowheads). D: Four major chemosensory target areas (1–4) can be distinguished. An "atypical" projection from Gr21a-Gal4 labeled TO neurons stays apart from these areas (asterisk). See text for further details. The sense organs providing input for each of these areas are given on the right. E,F: Projections of Gr2a-Gal4 and Gr66a-GFP labeled neurons, respectively, as deduced from Figures 2 and 3.

Using the Gal4-based approach in combination with the Flp-out strategy (Wong et al., 2002), we investigated the connectivity of the primary larval gustatory center in the SOG. Essentially, we compared the central projection patterns of GRNs belonging to different organs or having potentially different response profiles. Our data suggest a similar but not identical organization of the larval taste center compared to its adult counterpart. Apart from information about primary taste neurons, we also collected examples of putative second-order taste neurons. Other interesting candidate taste interneurons are described in a companion article (Bader et al., 2007).

MATERIALS AND METHODS

Fly strains

Drosophila stocks were raised on standard cornmeal medium at room temperature; CantonS (CS) was used as a wildtype control strain. Transgenic P[GAL4] lines used were Gr2a, 21a, 22f, 28be, 32a, 47a, 66a, (Scott et al., 2001; Wang et al., 2004), Gr5a, 8a, 22b, 22e, 22f, 28be, 32a, 59b, 59e, 59f, 64a, 64e, 66a (Dunipace et al., 2001; Thorne et al., 2004), and PPK 6, 10, 11, 12, 19 (Liu et al., 2003a). As a reporter line, we used UAS-mCD8:GFP (Lee and Luo, 1999). Larvae for the clonal analysis were obtained by crossing males of a given GAL4 line with virgins hsFLP;CyO/Sp;UAS>y+ CD2>CD8:GFP (Wong et al., 2002). For simultaneous labeling of different receptors, we crossed the males mentioned before with virgins of the genotype w-; UAS-CD2; Gr66a-I-GFP or w-; SP/CyO; Gr66a-I-GFP, UAS-CD2. We obtained these flies by combining the Gr66a-I-GFP/TM6 stock (Wang et al., 2004) and the CyO/UAS-CD2 and UAS-CD2 (III) stocks (Bloomington Stock Center, Bloomington, IN). For behavioral studies, we crossed UAS-Gcamp56; UAS-VR1E600K; TM2/TM6 (Marella et al., 2006) virgins to Gr66a-Gal4 or CS males or males of the same UAS line to virgins GH86 or CS.

Clone induction

FLP recombinase was induced by placing tubes containing larvae 1–2 days after egg laying (AEL) in a water bath maintained at 37°C for 1 hour (Gr-Gal4 clones) or 50 minutes (MJ94 clones).

Immunofluorescence

Antibody staining was adapted from an earlier protocol (Ramaekers et al., 2005). Briefly, young third instar larvae (72–96 hours AEL) were predissected in phosphate buffer (PB; 0.1 M, pH 7.2). The brains attached to the body wall were fixed for 20 minutes in PB containing 3.7% formaldehyde and subsequently rinsed in PBT (0.3% Triton X-100 in PB). They were further dissected and placed for 2 hours in PBT in 5% goat serum (NGS) at room temperature for blocking. Subsequently, they were incubated with a cocktail of primary antibodies overnight at 4°C. Primary antibodies included two neuropile markers: the mouse monoclonal anti-ChATB1 (dilution 1:500; Hybridoma Bank, University of Iowa, Iowa City, IA), and nc82 (1:20; A. Hofbauer, University of Regensburg, Germany). In addition, we used rabbit polyclonal anti-GFP (1:1,000; Molecular Probes, Eugene, OR; A6455) and mouse monoclonal antirat-CD2 (1:100; Serotec, Düsseldorf, Germany, MCA154R). After several rinses in PBT, samples were incubated overnight in PBT-NGS with the secondary antibodies (antirabbit Alexa 488-conjugated and antimouse Cy3-conjugated, diluted 1:200; Molecular Probes). Finally, brains were mounted in Vectashield (Vector Laboratories, Burlingame, CA), with nail polish used as spacer. The central nervous system (CNS) was mounted with the ventral nerve cord on top.

Anti-ChATB1 was raised by injection of extracted bacterially expressed *Drosophila* dChAT protein and was

shown to react with a single band at the position of ≈80 kDa in crude fly head samples (Takagawa and Salvaterra, 1996); nc82 was raised in mouse by injection of *Drosophila* head homogenate and which identifies a protein of 190 kDa in Western blots of homogenized *Drosophila* heads that was identified as Bruchpilot, a protein present in chemical synapses (Wagh et al., 2006). Anti-GFP was raised against GFP isolated directly from *Aequora victoria,* and antirat-CD2 was raised in mouse against activated T-helper cells from rat and was shown to recognize the rat CD2 cell surface antigen, a 50–54 kDa glycoprotein expressed by thymocytes and mature T cells (Whiteland et al., 1995). Both antibodies recognize the ectopically expressed GFP and CD2 proteins, respectively, as demonstrated by the absence of labeling in wildtype brains (data not shown). Secondary antibodies were raised in goat.

Image acquisition and processing

Images of the peripheral nervous system were taken by using a fluorescence microscope (Leica DM R) equipped with a CCD camera. Stacks of confocal images at 0.93 μm focal plane spacing were collected with a Biorad (Hercules, CA) MRC 1024 confocal microscope and Laser Sharp image-collection software. Images were then processed with ImageJ freeware (http://rsb.info.nih.gov/ij/index.html), curves (input to output options) were readjusted for each color independently but always on the whole picture. The intensity of unspecific background staining was lowered using the "dust and scratches" filter in Adobe Photoshop (San Jose, CA) for Macintosh 7.0 software.

Behavioral tests

Behavioral tests were performed using a modified previous protocol (Lilly and Carlson, 1990). Petri dishes separated in two halves with a plastic bridge (Greiner 635102) were filled first on both sides with 24 mL of agar, in order to minimize the required amount of tastant. After drying the agar, either 7 mL of plain 1.5% agarose were poured on the control (C) side, or agarose mixed with tastant on the stimulus (S) side, respectively. The second halves of the plates were poured 5–10 minutes later with the other type of agar. The central region was simultaneously filled with the second agar type in order to get a flat surface. The plates were then dried for 1 hour. Plates are thus divided into two halves containing agar alone and agar with tastant, respectively, the middle portion containing either type of agar in a random manner. To avoid any bias toward the type of agar in the center region and the sequence of pouring, in 50% of the cases the C side, and in the other 50% the S side, was poured first.

Three-day-old larvae (AEL; reared at 25° on a 12/12 light dark cycle) were collected using sugar solution and then rinsed in tap water. About 50 larvae were distributed along the separating plastic bridge and allowed to freely move on the entire plate. After 15 minutes in total darkness, a photo of the dish was taken and larvae were counted. A response index was calculated [RI = (Ns – Nc) / (Ns + Nc)], where Ns and Nc refer to the numbers of larvae present on stimulus and control areas, respectively. Animals found at a distance of less than 0.5 cm from each side of the bridge were discarded. Multiple tests were done in parallel; half of the plates were turned by 180° to compensate for any other unexpected context effect.

RESULTS

In this article we describe the sensory projections in the primary taste center of *Drosophila* larvae. Our observations allowed us to delimit the target region in the SOG dealing with gustatory information, and furthermore to define subareas that may be associated with different taste properties. We made use of the genetic tools provided by this species, studying the expression patterns of different Gal4 reporter lines, namely 1) 20 lines driven by different Gr promoters (for some Gr promoters also multiple lines), lines whose adult expression was previously reported (Dunipace et al., 2001; Scott et al., 2001; Bray and Amrein, 2003; Thorne et al., 2004; Wang et al., 2004); 2) five Ppk-Gal4 lines, including three previously described (Liu et al., 2003a); and 3) the enhancer trap lines GH86 (Heimbeck et al., 1999) and MJ94 (Gendre et al., 2004) that were both shown to be expressed in GRNs.

Using the UAS-CD8:GFP reporter line, we visualized the expression of these lines in the peripheral and central nervous system (Figs. 1A–C, 2). The widespread expression pattern of certain Gal4 lines was dissected by tagging single cells via the Flp-out technique (Wong et al., 2002). In such preparations, one or a few of the Gal4 expressing cells were labeled by UAS-CD8:GFP, whereas the rest of the Gal4-expressing cells were labeled by UAS-CD2 (Fig. 3A–D,L–O). Furthermore, using CD2 as a reporter, we investigated the expression of different Gal4 lines in the background of Gr66a-GFP. Studying coexpression allowed us to compare the location and morphology of sensory terminals deriving from different sensory neurons (Fig. 3E–K). Finally, we describe a putative second-order gustatory neuron labeled in the GH146 Gal4 line (Fig. 3Q–S). Our results are schematized in Figures 1 and 4.

Peripheral expression

The *Drosophila* larva comprises about 90 pairs of GRNs, located in different sensory organs in the head and on the body wall (Table 1). The major cephalic chemosensory organs, the DO, TO, VO, and the four pharyngeal organs (Fig. 1A,B) (cf. Singh and Singh, 1984; Python and Stocker, 2002) contain multiple sensilla. Many of them, e.g., those of the TO, can be distinguished by their cuticular protrusions (Fig. 1C); this allowed us to identify the type of sensillum to which the labeled neurons belonged (Fig. 2, insets).

Of the 20 Gr-Gal4 lines tested, five showed expression neither in larvae nor in adults and five additional lines were expressed only in the adult taste system (Table 1). However, the 10 remaining Gr-Gal4 lines showed expression in both the larval and adult gustatory system (Table 1). Three of the five Ppk lines used were expressed in the larval taste system (Table 1), but in contrast to a previous report (Liu et al., 2003a), we did not detect expression of Ppk19 in taste organs. The number of labeled GRNs in the Gal4 lines studied varied from 1 to 18 pairs (Table 1). The enhancer trap line GH86 showed expression in more than 30 GRNs (Table 1; Fig. 4), in some ORNs and in certain nonneuronal cells, but lacked expression in central neurons (Heimbeck et al., 1999). The MJ94 line showed expression in many if not all sensory neurons—apparently including the entire set of GRNs—but no expression in central neurons (Gendre et al., 2004).

With the exception of Gr32a-Gal4, the expression patterns of the Gal4 lines were consistent from animal to animal (although expression levels varied to a certain

http://doc.rero.ch

extent). In addition, different inserts of the same Gr-Gal4 construct revealed similar patterns in the majority of cases. Exceptions were Gr22b-Gal4 and Gr66a-Gal4; in the former, only one of the two strains (B7) labeled VPS neurons (Fig. 2G and data not shown). For Gr66a-Gal4, one line (from K. Scott) showed less expression than the other one (from H. Amrein), the latter being similar to the Gr66a-GFP line (compare Fig. 2B,C). Analogous pattern differences between these two lines were previously reported in adult flies (Wang et al., 2004). None of the lines studied displayed asymmetrical expression patterns. However, small differences in the level of expression were sometimes noticed between neurons on the left and right side (Fig. 3F and data not shown) and for particular cell types. For example, in Gr2a-Gal4 staining was weaker for TO and VO neurons than for other neurons (Fig. 1B).

In Gr-Gal4 lines expression was rare outside the gustatory system and was completely absent from the olfactory organ. Remarkably, Gr21a-Gal4, which labels olfactory neurons in the adult antenna (Suh et al., 2004), showed expression in one TO neuron, but not in olfactory neurons of the DO (Fig. 2F). In contrast, Gr68a-Gal4 labeled non-neuronal cells of the TO, in addition to its expression in two VPS neurons (data not shown). Similarly, Gr22e-Gal4 labeled cells belonging to the TO, VPS, DPS, and DPO; these cells lacked axons and should thus be nonneuronal (Fig. 2J). Gr22e-Gal4 showed also expression in multidendritic neurons in head, thoracic, and abdominal segments (data not shown). As expected from the ionic channel nature of Ppk proteins, and as reported previously (Liu et al., 2003a), Ppk-Gal4 lines showed expression in various body parts apart from the gustatory system. For instance, Ppk11-Gal4, that labeled three TO neurons, also showed strong expression in the tracheal system, obscuring neuronal patterns in the CNS (data not shown).

Using CD2 as a reporter, we also studied the expression of different Gal4 lines in the background of Gr66a-GFP, a line that labels a relatively large proportion of GRNs (18 pairs: one-fifth of GRNs; Fig. 4). As expected from the situation in the adult (Thorne et al., 2004; Wang et al., 2004), Gr28be-, Gr22b-, and Gr22e-Gal4 lines showed expression in a subset of Gr66a-GFP-positive GRNs (Fig. 4). More surprising, Gr68a-Gal4 and even Ppk12-Gal4 showed coexpression with Gr66a-GFP (Fig. 3K). In contrast, Gr21a-Gal4, Gr2a-Gal4, Gr59f-Gal4, and Ppk6-Gal4 showed no overlap with Gr66a-GFP expression (Fig. 4). For another three Gal4 lines, coexpression with Gr66a-GFP was not checked. Together, these seven lines stained at least 11 and at most 17 GRNs that are not included in the Gr66a-GFP pattern (depending on their relative coexpression in TO neurons, see Table 1). About one-third of GRNs were thus labeled by the Gr-and Ppk-Gal4 lines studied (29–35, from the total of 90). Interestingly, the GH86 line was expressed in Gr66a-GFP-negative cells (Fig. 3I,J, periphery not shown), suggesting that the GH86 pattern covers another third of GRNs (Table 1; Fig. 4).

Central projections of GRNs

In order to define landmarks for limiting the SOG, we used the neuropile marker anti-choline-acetyltransferase (ChAT; Fig. 2A1); this allowed us to accurately map the projections of the different GRNs labeled by different Gal4 lines (Fig. 2). In the cases of Gr2a-Gal4 and Gr66a-Gal4 that labeled neurons from multiple organs (Fig. 2A,B), we used the Flp-out technique (Fig. 3A–D) to associate each terminal projection with its proper sensory organ (Fig. 1E,F). Then, studying the projections of different Gal4 lines or of the GH86 line in the background of Gr66a-GFP allowed us also to assess the spatial relations of two sets of projections (Fig. 3E–J). Finally, in order to see if the GRNs not expressed in those different Gal4 lines could show other types of projections, we generated Flp-out clones in MJ94, which is not only expressed in all GRNs but also in sensory neurons of other modalities (Fig. 3L–O). Because the afferent projection patterns appeared to depend mainly on their peripheral origin, the following description of taste afferents is grouped according to the different peripheral nerves, starting with the most ste-

Fig. 2. Expression patterns of Gr-Gal4 and Ppk-Gal4 lines, visualized by UAS-CD8:GFP reporter labeling (or direct GFP expression in Gr66a-GFP: C). The panels show the sensory projection patterns in the SOG (stained by anti-GFP; green) in the background of anti-ChAT staining (magenta). Insets (except A1/A3) refer to the corresponding GFP expression patterns in the periphery (expression in additional sensory organs is indicated). The SOG is shown horizontally, with anterior on top. The Z stacks of the confocal images (comprising 22–28 μm) include the entire depth of the projections (except in H). Insets in A1/A3 display the projection of only the five ventralmost sections of the stack; insets in B,D,E,F refer to the TO and its sensilla, and the remaining insets show the entire larval head with the labeled sensory organs (asterisks: mouth hooks). Lines, whose names are shown in italics, are coexpressed with Gr66a-GFP. Refer also to text and to Figure 1 for description of "regular" projections and target areas. **A1,2,3:** Anti-ChAT staining, Gr2a pattern, and merged image, respectively. A1: Stronger anti-ChAT staining occurs posterior to MN and LbN entries (see also B,D). Arrows mark the entry points of the different nerves in the SOG; the antennal lobe position (AL, outline) is identifiable in the ventral sections (inset). A2: Weakly labeled terminals of MN afferents (TO and VO neurons, arrows) are adjacent to those of LrN afferents (DPS neurons, arrowheads). Small symbols in the inset refer to dendrites, large ones to cell bodies. (A3) Projections from ventral pits and nonolfactory DO neurons both target *area 3* (arrows). DPS terminals are located at the anterior SOG neuropile border (arrowhead, see inset) in *area 4* (Fig. 1E). **B:** Gr66a-Gal4 (from K. Scott) labels "regular" MN and LrN projections in *area 2*; note absence of staining at midline (arrowhead). An "atypical" neuron of a dorsolateral TO sensillum (inset: TODO) projects via the AN into *area 4* (arrow). **C:** Gr66a-GFP (used in coexpression studies) shows more widespread pattern in pharyngeal sensilla than Gr66a-Gal4 (B, see inset and also Fig. 3K). The projection patterns are similar as in B, apart from the presence of fibers deriving from the LrN that cross the midline (arrowhead). **D,E:** MN projections from TO neurons labeled by Gr28be (D) and Gr59f (E) are similar, except that the latter extend more laterally (arrowhead). **F:** Distinct projection of another TO neuron revealed by Gr21a. **G:** Gr22b shows LbN projections ending close to LrN terminals in *area 2*. **H:** Overlapping terminals of "regular" LbN and MN projections in *area 2*, labeled by Ppk6. The overlap (arrows) is best demonstrated in a single optical section (inset 2, but see also supplementary data online). The most dorsal part of the LbN nerve projection is not included in this stack (arrowheads). **I:** Overlapping "regular" LrN and MN projections in *area 2*, labeled by Ppk12. Widespread expression of Ppk12 (inset) may hide expression in other GRNs, which is suggested by the multifiber appearance of terminals in *area 1*. **J:** Gr22e labels many neural and nonneuronal cells (inset: only neuronal cells are marked). In addition to projections similar to C, extra projections in the ventral nerve cord (arrow) deriving very likely from multidendritic neurons are stained. Scale bars = 50 μm.

http://doc.rero.ch

http://doc.rero.ch

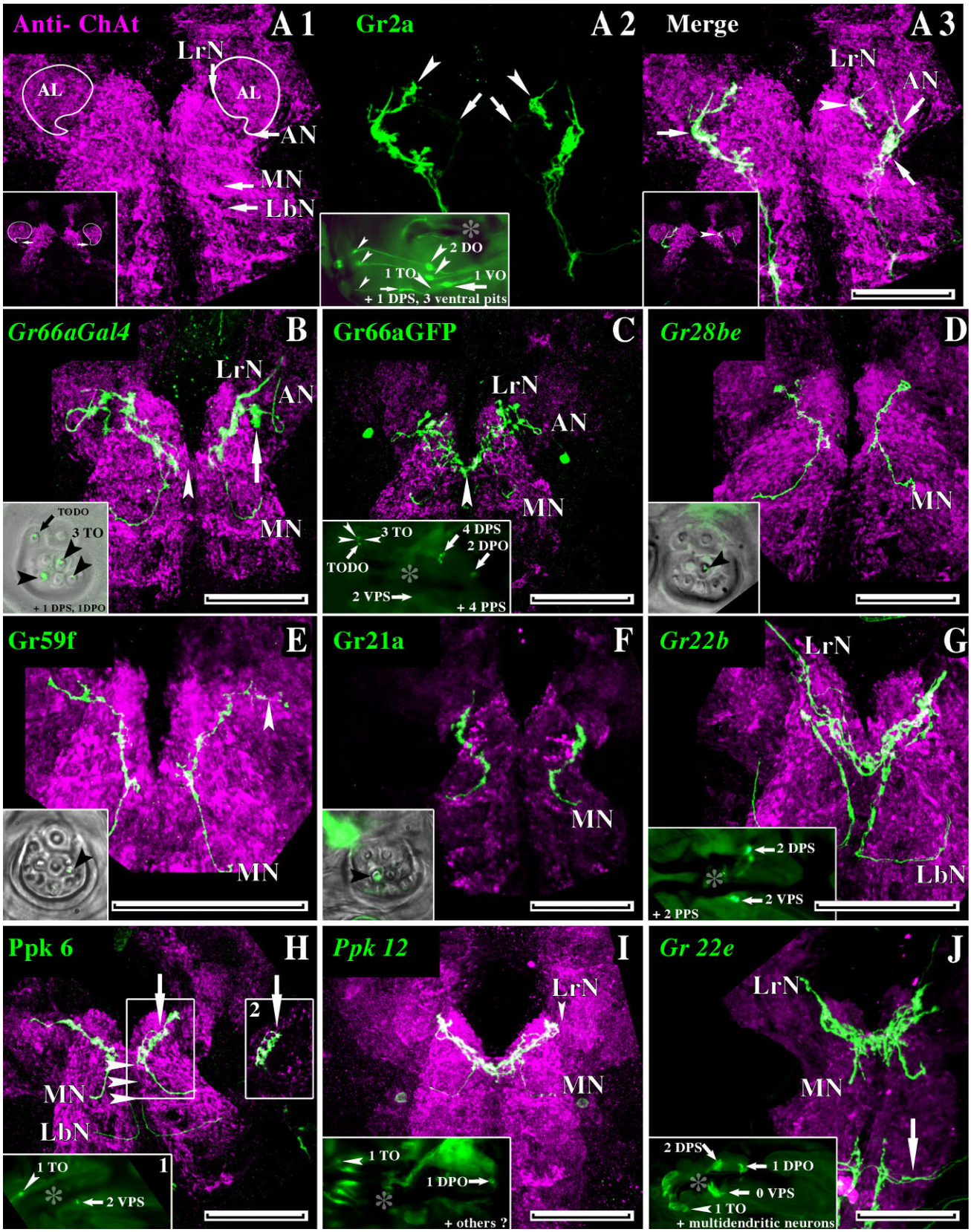

Figure 2

http://doc.rero.ch

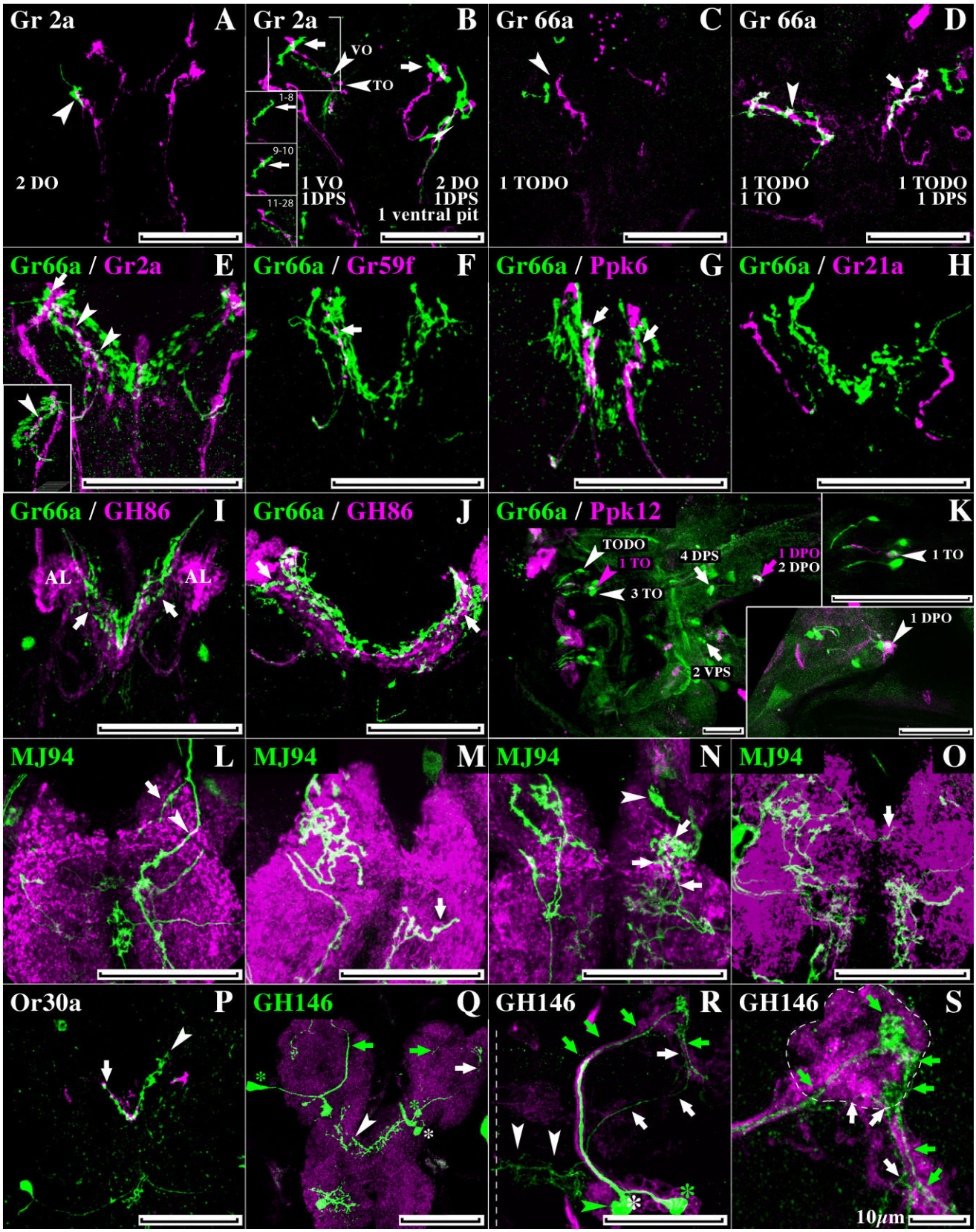

Figure 3

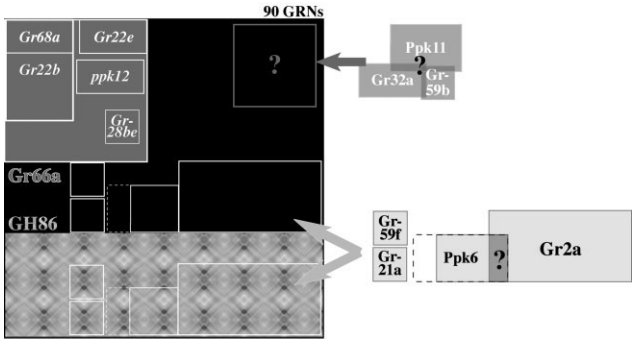

Fig. 4. Diagram showing proven and suggested patterns of coexpression of the different Gal4 lines used, as well as the proportion of GRNs labeled. Evidence of coexpression was obtained by double labeling and visualization of the periphery (cf. Fig. 3K). Square size corresponds to the numbers of labeled GRNs (i.e., Gr28be representing one pair of GRNs). From the total of 90 GRNs, one-fifth are labeled by Gr66a (dark gray) and one-third by GH86 (patterned area). Coexpression of the seven GRNs labeled by Ppk11, Gr32a, and Gr59b with other lines was not assessed (gray squares and question mark). Lines labeled in light gray are not coexpressed with Gr66a, but may (or may not) be coexpressed with GH86 (white squares in the black and patterned areas). The TO neuron labeled by Ppk6 might be identical to the one labeled by Gr2a (question mark), but not to those labeled by Gr59f (which is from a different TO sensillum) and Gr21a (which has a particular brain projection). The black part represents unlabeled GRNs, studied in MJ94 clones. Coexpression between lines that are coexpressed with Gr66a-GFP is not shown (except for the known coexpression of Gr68a, Gr22b, and Gr66a in two VPS neurons).

reotyped ones. We numbered projections areas from medial to lateral (Fig 1D), irrespective of their sequence of appearance in this description.

Maxillary nerve (MN). MN projections derived from GRNs in the TO and VO (Fig. 1A); they remained on the ipsilateral side of the SOG throughout. All MN projections showed similar terminal patterns (Fig. 2A–E,H–J) independent of the Gal4 line studied (Fig. 3E–G,I,J) and irrespective of whether the afferents came from the TO or the VO (Fig. 3B). An exception was the TO neuron labeled by Gr21a-Gal4 (see below). "Regular" projections were best described in Gal4 lines showing expression only in one TO neuron (Fig. 2D,E). After entering the SOG quite posteriorly, the MN afferents passed horizontally toward the midline. Upon arriving in the neuropile proper (about one-third from lateral to medial), they turned anteriorly and slightly dorsally. In the middle of the SOG neuropile (from posterior to anterior) they bent laterally and ventrally again, establishing terminal extensions, in a target region that we called *area 2* (Fig. 1D). The exceptional projection of the TO neuron labeled by Gr21a-Gal4 turned sooner anteriorly and terminated more posteriorly than the regular TO neurons (Figs. 2F, 3H).

Labral nerve (LrN). LrN projections that entered the SOG on its anterior part (Fig. 2A1,G), comprised GRNs from the DPS, DPO, and PPS (Fig. 1A). We found both ipsilateral (Figs. 2A,B, 3O) and bilateral projections (Fig. 3P, see also Fig. 2C,G,I,J). Most of the LrN afferents followed those from the MN in *area 2* (Fig. 2I) and generally continued to the midline region into *area 1* (Fig. 1D, but see Fig. 2B). In the majority of cases they then seemed to target the contralateral *area 2* (Fig. 3P, but see Fig. 3O). An exception was one DPS fiber labeled by Gr2a-Gal4 (Figs. 2A2, arrowheads; 3B,E, arrows, see also Fig. 3N, arrowhead), which produced an ovoid-shaped cluster of terminals at the neuropile border of

Fig. 3. Clonal analysis (A–D) and double labeling studies (E–K) of different Gr-Gal4 and Ppk-Gal4 lines, Flp-out analysis of the MJ94 line (L–O), and dissection of the putative second-order taste neuron labeled by GH146 (Q–S). Z confocal stacks (depth 20–28 μm; 35 μm in Q,R) of sensory projections labeled with anti-GFP (green) and on top of (magenta) anti-CD2 (A–K,P,R,S) or the neuropile markers anti-ChAT (L–O) and nc82 (Q). Horizontal views, anterior on top. **A–D:** Clonal analysis of Gr2a and Gr66a permits linking the different projections with their organ of origin (cf. Figs. 1E,F, 2A,B). Neurons that underwent Flp-out are labeled by GFP, nonflipped neurons by CD2. A: The DO neurons target *area 3*. B: This multiple clone shows the terminals of a VO neuron close to those of a TO neuron (labeled by CD2, arrowheads) in *area 2*, as well as DPS projections in *area 4* (arrows) ventral to the TO projections (illustrated in projections of selected optical sections (insets); some overlap remains in sections 9–10). C: The TODO neuron terminates near the "regular" TO projection in *area 4* (arrowhead). D: The terminals of a single TO neuron (arrowhead) and of a DPS neuron (arrow) overlap with CD2 labeled pharyngeal projections in *area 2*. **E–K:** Gr66a-GFP expression (green; cf. Fig. 2C) related to the expression of other Gal4 lines labeled by CD2 (magenta; cf. Fig. 2A,E,F,H,I). E: Terminals of TO and VO neurons labeled by Gr2a are in close proximity with those of a Gr66a-GFP labeled TO neuron in *area 2* (arrowheads), best illustrated by a 150° turn (inset). A Gr2a-labeled DPS neuron projects slightly more medially than the TODO neuron labeled by Gr66a in *area 4* (arrow, see Fig. 1D). F,G: Projections of a Gr59f-labeled TO neuron (F) and of TO and VPS neurons labeled by Ppk6-Gal4 (G), are in close proximity to the Gr66a-GFP projections in *area 2* (arrow). H: The TO projection labeled by Gr21a extends more posteriorly than the Gr66a-GFP projections. I,J: The projections labeled by the GH86 line overlap with those of Gr66a-GFP in the lateral part of *area 2* (arrows), but are slightly more posterior in the medial part and in *area 1*. K: Peripheral expression of Gr66a-GFP and Ppk12 (cf. Fig. 2B,I). Higher magnification (insets) shows GFP expression in CD2 labeled cells (arrowheads). Because CD2 is membrane-tagged while GFP is cytosolic, few white areas are visible. **L–O:** Flp-out clones generated in the MJ94 line. Projections crucial for our interpretation are marked (see text). L: Two afferents of unknown origin carried by the LrN project to the SOG (arrow) and the ventral nerve cord (arrowhead). M: The projection of a head multidendritic neuron (arrow) enters via the MN and extends to the ventral nerve cord. N: Two neurons, very likely from the TO, project posterior to *area 2* (arrows) and a DPS neuron terminates similar to the one labeled by Gr2a in *area 4* (arrowhead, cf. Fig. 2A). O: An afferent from the LrN, perhaps from the DPS, projects to the *area 1* but does not extend contralaterally (arrow). **P:** Flp-out clones of Or30a-Gal4, showing extra expression in a pair of DPS neurons, which exhibit a bilateral projection (arrow; arrowhead: nerve entry). **Q–S:** The GH146 line labels a putative gustatory interneuron (asterisks: cell bodies) that projects to the lateral horn and the mushroom bodies. Arrowheads and arrows indicate possible dendritic and axonal portions, respectively. Olfactory PNs (green signs) and the putative gustatory interneurons (white signs) are stained by CD8 (green). Q: A GH146 clone on top of nc82 labeling. Apart from an olfactory PN in each brain hemisphere, the right putative gustatory interneuron is labeled and shows arborization in the contralateral SOG (arrowhead). R,S: An olfactory PN and a putative gustatory interneuron on top of the entire GH146 pattern (in magenta). R: The right brain half is shown (midline stippled). S: Higher magnification of the putative output region. Both types of neurons project to the mushroom body calyx (stippled contour) and to the lateral horn (region posterolateral to the calyx), terminating close to each other in both areas. Scale bars = 50 μm.

http://doc.rero.ch

TABLE 1. Number of Cells in Taste Sensilla Labeled by the Gal4 Lines Used

Lines	TO	DO	VO	DPS	DPO	PPS	VPS	Additional Expression
Gr66a-GFP	**4**	**1**		**6**	**2**	**4**	**2**	
Gr66a[1] (Scott's line)	2 (1)	1 (0)		1	1			
Gr28be[1]	1				1			
Gr22b				1	1	2	2	
Gr22e	1				1			+ multidendritic, + nonneuronal TO
Gr68a							2	+ nonneuronal TO
Ppk12	1				1			
Ppk6[2]	**1**						**2**	
Gr21a[1]	**1**							
Gr2a[1]	**1**	**2**	**1 (0)**	**2**				+ 3 ventral pits
Gr59f	**1**							
Ppk11	**3**							
Gr59b	**1**							
Gr32a[1]	**1? (1)**			1? (0)				
Total labeled	**7–13**	**3**	**1**	**8**	**2**	**4**	**4**	**Total: 32–38**
No. of taste cells	**23**	**11**	**4**	**18**	**5**	**6**	**16**	**Total: 90**
GH86	19	?	2	9–13	?	?	?	**Total > 30**
Not expressed: Gr8a, Gr10a, Gr22a, Gr22f, Gr63a, Ppk10, Ppk19[2]								
Expressed only in adults: Gr5a, Gr47a, Gr59e, Gr64a, Gr64e								

See text for abbreviations. Lines in italics show expression in a subset of cells labeled by Gr66a-GFP (coexpression of Ppk11, Gr59b, and Gr32a was not assessed because of weak or variable expression). Numbers in parentheses refer to prior studies.
[1]Lines described in Scott et al. (2001).
[2]Lines described in Liu et al. (2003a).
The total number of taste cells in sensilla were deduced from Python and Stocker (2002) and Gendre et al. (2004). Numbers of cells labeled by GH86 were deduced from Heimbeck et al. (1999).

http://doc.rero.ch

the SOG lateral and ventral to *area 2* (Fig. 3B, insets), inside *area 4* (Fig. 1D).

Labial nerve (LbN). LbN projections derived from GRNs in the VPS (Fig. 1A); they remained ipsilateral. Fibers entered the brain more posteriorly than those from the MN (Fig. 2H) and then traveled at the midline, more dorsally than all other projections (Fig. 2H). They finally joined and got intermingled with pharyngeal (Fig. 2G) and TO projections (Fig. 2H, inset, see supplementary data online) in *area 2* (Fig. 1D).

Antennal (AN) and thoracic nerves. Only a few Gal4 lines showed expression in GRNs associated with the AN or thoracic nerves. Hence, whether the observed projection patterns are the common ones for these neurons or rather exceptional cases remains unknown. Specifically, Gr2a-Gal4 labeled DO neurons and thoracic neurons (Fig. 2A), whereas Gr66a-Gal4 labeled one of the three neurons associated with the DO but extending their dendrite in a TO sensillum (referred to as TODO neuron, Fig. 2B,C). AN projections comprised both DO and TODO neurons (Fig. 1A), which established distinct but always ipsilateral terminals. Two DO neurons labeled by Gr2a-Gal4 (Figs. 2A, 3A,B) followed olfactory receptor axons along the AN, but continued posteriorly instead of passing into the antennal lobe (Fig. 3A3 inset, arrow). They ended in a small cluster at the neuropile border in *area 3* (Fig. 1D,E), posterior to *area 2* and *area 4*. The TODO neuron labeled by Gr66a-Gal4, in contrast to the DO neurons mentioned above, turned medially at the entrance of the AL and ended in an ovoid target area at the SOG neuropile border (Figs. 1D,F, 2B, arrow), just lateral to the exceptional DPS projection in *area 4* (Fig. 3C–E). Thoracic projections from ventral pit organs (labeled by Gr2a-Gal4) established ipsilateral terminals in the ventral nerve cord and traveled further anteriorly to end adjacent to, but not intermingled with, DO projections (Figs. 1E, 3A).

Projections from other sensory modalities

Our data also provide information about afferents mediating other modalities than taste, such as smell, touch, stretch, temperature, or humidity (Stocker, 1994; Liu et al., 2003b). For example, olfactory receptor neurons projecting to the larval antennal lobe (Fishilevich et al., 2005; Ramaekers et al., 2005) (Fig. 2A, inset) were labeled by both MJ94 and GH86 lines (Fig. 3I). Moreover, Gr22e-Gal4 demonstrated that multidendritic neurons—thought to be pain receptors (Tracey et al., 2003)—project exclusively to the ventral nerve cord (Fig. 2J, arrow). Furthermore, as shown in clones of MJ94, which labels sensory neurons of different modalities, some afferents carried by the MN and LbN nerve projected to target areas in the ventral nerve cord (Fig. 3L,M). These results suggest that the SOG might be devoted principally to taste processing (see Discussion).

Functional testing

The central projections of GH86 and Gr66a-GFP labeled GRNs were essentially similar, adjacent to each other along their path. However, the target area of GH86 appeared to be slightly more posterior, although overlap was found in the lateral portion of the SOG (Fig. 3I,J). To check whether the two sets of GRNs might correspond to functionally different categories, we took advantage of the Gal4/UAS system in order to drive expression of a modified version of the mammalian capsaicin receptor (Marella et al., 2006). This technique allows one to artificially activate GRNs by capsaicin, which normally does not drive any behavioral response in chemotaxis assays (but see Discussion). Thus, testing larval behavior toward capsaicin permits one to assess the basic function of these cells. In our experiment, control larvae (CS, heterozygous GH86, GR66a-Gal4 and UAS-CapsR) did not react to capsaicin (Fig. 5). However, the expression of the capsaicin receptor in Gr66a-Gal4 cells induced aversion toward capsaicin, suggesting that these cells normally respond to aversive stimuli. In contrast, the expression of the receptor in GH86-positive cells neither led to attraction nor to repulsion, suggesting that functionally different cells are labeled in this line (Fig. 5, see Discussion).

Second-order taste neurons

To search for putative second-order gustatory neurons, we studied the expression patterns of a number of Gal4

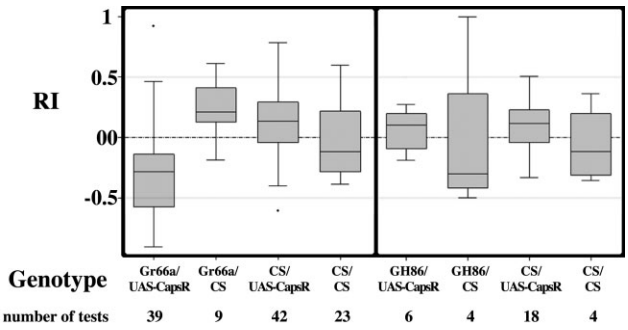

Fig. 5. Behavioral responses of larvae of different genotypes toward capsaicin. Positive scores indicate attraction, negative ones repulsion. Horizontal lines, boxes, and whiskers indicate, respectively, median, quartiles, and extreme values, excluding outliers (represented as dots, outliers are data points which are beyond 1.5 times the interquartile range above the third quartile or below the first quartile). Left: Double heterozygous Gr66a/UAS-CapsR larvae avoid capsaicin ($P < 0.01$), whereas controls do not respond at all. Right: Double heterozygous GH86/UAS-CapsR larvae do not respond to capsaicin, similar to control larvae.

enhancer trap lines that show labeling in the SOG. A candidate gustatory interneuron was identified in the GH146-Gal4 line, which is known for its expression in olfactory projection neurons (Stocker et al., 1997; Heimbeck et al., 2001). This novel neuron showed contralateral projections in the SOG, which cover a large area (3–7 μm) (Fig. 3Q, arrowhead). Expressing the presynaptic reporter synaptobrevin-GFP did not label these projections, suggesting that they might be postsynaptic (data not shown). Another process of this neuron—perhaps representing an output connection—extended via a lateral path to the lateral horn and further to the mushroom body calyx (Fig. 3R,S). In both regions arborizations were present, partially overlapping with the terminals of olfactory projection neurons. Other good candidates of gustatory interneurons are the *hugin*-expressing neurons (Melcher and Pankratz, 2005); a detailed study of their anatomy is provided in the accompanying article (Bader et al., 2007).

DISCUSSION

By using Gr-Gal4, Ppk-Gal4, and enhancer trap lines, in combination with the Flp-out technique, we extended previous work about the projections of GRNs in the CNS of the *Drosophila* larva (Scott et al., 2001). We described about one-third of the estimated 90 larval GRN projections individually and studied another third more globally using the GH86-Gal4 line (Fig. 4). Also, we visualized many of the remaining GRN projections with the MJ94-Gal4 line. We thus believe that our interpretations are based on a rather complete and detailed description of the afferent morphologies. We observed that the sites of afferent terminals in the SOG were correlated primarily with their nerve proper, and therefore with their sensory organ of origin. This allowed us to delimit subareas in the SOG, corresponding to the origin of afferents (Fig. 1D). However, we also found circumstantial indications for a subtle functional division of the SOG (see below). Furthermore, studying the patterns of Gal4 lines together with Gr66a-GFP expression provided evidence about GR coexpression and possible overlap of the terminals of different GRNs. Finally, observations about putative second-order taste neurons enabled us to hypothesize about the principles of gustatory coding in *Drosophila* larvae.

SOG architecture

By comparing the site of terminal projections in the SOG with their peripheral origin, which we assessed by identifying cell bodies and dendrites, we established that neurons projecting through the same nerve show essentially similar terminal patterns (Fig. 1D). Also, we were not able to recognize consistent differences in the projections of Gr66a-GFP and those of Gr-Gal4 or Ppk-Gal4 lines when afferents traveled in the same nerve (an exception was Gr21a-Gal4; see below). We showed that the majority of these projections are very close to each other (Fig. 3B,D; supplementary data online); this suggests that there is little spatial segregation between projections from neurons expressing different receptors. However, we do not know whether the selection of patterns visualized is biased to some extent by the Gal4 lines available (see below). Yet the projection patterns relate mainly to the nerve taken by a particular afferent and, accordingly, to the segmental origin of the GRN. This is reminiscent of the gustatory projections in larval *Manduca sexta*, which stay in the neuromeres corresponding to the segmental origin of the organs (Kent and Hildebrand, 1987).

However, three exceptions were found. First, GRN afferents traveling via the AN show at least two different kinds of terminals: while neurons deriving form nonolfactory sensilla of the DO terminate in *area 3*, TODO neurons target *area 4*. Second, a TO neuron labeled by Gr21a-Gal4 projects more posteriorly than the remaining TO neurons. Closer inspection revealed that these terminals remain outside the antennal lobe, in contrast to a previous report (Scott et al., 2001). Since this neuron was shown to respond to CO_2 (Faucher et al., 2006), this particular target region may be devoted to the sensation of this particular chemical. Third, projections from pharyngeal sensilla do not belong to one homogeneous class: we found projections covering only the ipsilateral *area 2*, projections ending in *area 1*, and projections showing bilateral terminals. Moreover, certain DPS neurons terminate in *area 4*. The functional implications and the developmental constraints leading to these differences remain to be investigated.

Based on Gr2a-Gal4 projections, Scott et al. (2001) reported discrete terminal regions for gustatory projections in the larval CNS. From our more complete description, we define four major target regions in the SOG (Fig. 1D). A midline *area 1* receives inputs exclusively from pharyngeal organs (DPS, DPO, PPS). A larger, more lateral *area 2* is defined by the convergence of inputs from both internal sensilla (including VPS) and external sensilla (TO, VO). A small posterior *area 3* appears to be the target of nonolfactory DO neurons and ventral pit neurons. However, because all evidence about *area 3* projections was collected in Gr2a-Gal4, it remains possible that this region is related to a particular chemical rather than to particular sensilla. An anterior lateral *area 4*, adjacent to the antennal lobe, accommodates the terminals of one or a few DPS neurons and of a TODO neuron. Finally, the GRN labeled by Gr21a-Gal4 has its own, specific target region posterior to *area 2*. As in the adult, the SOG can thus be divided in different regions that are targets of different organs. However, unlike adults (Stocker and Schorderet, 1981; Nayak and Singh, 1985; Shanbhag and Singh, 1992;

http://doc.rero.ch

Thorne et al., 2004; Wang et al., 2004), the projections from internal and external organs do not segregate but remain intermingled.

Interestingly, most of the pharyngeal projections seem to be bilateral, similar to the situation in the adult (Stocker and Schorderet, 1981; Rajashekhar and Singh, 1994). Terminals are sometimes restricted to *area 1*, but often extend to the contralateral *area 2*. In contrast, GRNs belonging to nonpharyngeal sensilla establish exclusive ipsilateral projections. An example is Gr66a-Gal4-labeled TO projections. This is very striking because adult Gr66a-Gal4 projections from the labial palp are clearly bilateral (Thorne et al., 2004). The reason for this disparity is unknown. Perhaps it is correlated with different functions of the two sensory organs. For maggots that live in a semiliquid environment, bitter taste information from the TO may help to navigate up or down a gradient, a behavior that may use laterality information. In contrast, Gr66a-Gal4-positive labellar GRNs may participate in food rejection, which very likely does not require spatial information. Compatible with such an interpretation, adult Gr32a-positive leg GRN (a subset of GR66a-positive cells) projections remain ipsilateral in the SOG (Wang et al., 2004). This suggests that they might be involved in chemotaxis in a bitter gradient.

SOG and nongustatory cues

In the blowfly, mechanosensory neurons were thought to target a specific region of the SOG (Edgecomb and Murdock, 1992). A similar segregation of the targets of mechanosensory neurons and GRNs is known from leg sensilla in *Drosophila* (see, for instance, Murphey et al., 1989). Our data show that multidendritic neurons, which may be involved in pain sensation (Tracey et al., 2003), project to the ventral nerve cord. Strikingly, we observed that some afferents from the MN or LrN also terminate in the ventral nerve cord. This suggests that certain nongustatory neurons associated with taste sensilla may have their targets outside the SOG. However, further studies will be required to clarify the sensory modalities involved and to answer whether the SOG receives direct mechanosensory input or not.

Evidence that temperature sensation may be encoded in the SOG is more compelling. TO neurons were shown to respond to heat (Liu et al., 2003b). Moreover, cells labeled by the GH86 line are necessary for thermotaxis (Liu et al., 2003b). It is thus likely that some of the TO neurons labeled by GH86, which we observed to project entirely into the SOG (Fig. 3I,J), are thermosensitive. Interestingly, a link between taste and temperature sensitivity was described at the molecular level. For instance, the mammalian capsaicin receptor appears to respond to heat, taste, and probably painful stimuli (Caterina et al., 1997). Similarly, in *Drosophila* the *painless* gene was shown to be involved in moderate thermal sensation, pain sensation (Tracey et al., 2003), and in the perception of isothiocyanate, a bitter-tasting chemical (Al-Anzi et al., 2006). Further evidence for links between taste, temperature, and pain sensation is provided by the expression of *painless* in the TO (data not shown; Tracey et al., 2003) and by the expected expression of the taste receptor Gr22e in pain-sensitive multidendritic neurons, as suggested by the Gr22e-Gal4 pattern.

Functional subdivisions?

Anatomical and functional evidence has shown that adult GRNs project to different target areas in the SOG, according to their receptivity to bitter or sweet compounds (Thorne et al., 2004; Wang et al., 2004; Marella et al., 2006). In these studies, Gal4 lines driven by the promoters of the trehalose receptor Gr5a and of the bitter receptor Gr66a served as marker lines. As mentioned, we did not find any obvious difference when comparing the projection patterns of different Gr-Gal4 and Ppk-Gal4 lines, with the exception of Gr21a-Gal4. However, since none of the three Gr5a-Gal4 lines that we tested showed any expression in larvae, our failure of detecting two distinct projection patterns might merely indicate that we had selected only bitter- and salt-sensitive GRNs, which together may project in a region different from the sugar-sensitive neurons. Indeed, GRNs labeled by GH86 that were suggested to mediate chemotaxis toward sugars (Heimbeck et al., 1999) appear to project more posteriorly than the majority of the GRNs labeled by Gr66a-GFP.

In order to correlate these subtle differences in projection with functional responses, we tested the basic sensitivity of the GRNs labeled by Gr66a-Gal4 or by GH86 via the UAS-capsaicin receptor approach (Marella et al., 2006). Thus, we measured chemotaxis toward capsaicin of larvae expressing a modified version of the mammalian capsaicin receptor in these two sets of cells (Fig. 5). Wild-type and other control larvae did not respond to this chemical in this assay, although there is evidence that adults may sense it (Al-Anzi et al., 2006). Larvae expressing the receptor via the Gr66a-Gal4 line provided by H. Amrein (which shows a similar expression pattern as Gr66a-GFP) were repelled by capsaicin. This suggests that normally these neurons respond to aversive stimuli. In contrast, driving expression of the capsaicin receptor with GH86-Gal4 elicited neither aversion nor attraction. Several explanations might account for this result. First, expression could have been too low to trigger responses in the neurons. However, this is not very likely because the levels of GFP expression driven by GH86-Gal4 and Gr66a-Gal4 appeared similar. Second, the natural sensation of capsaicin could prevent larvae from showing attractive behavior in this test, although it does not drive avoidance. This also seems unlikely since capsaicin does not prevent, but strengthens the attraction of adult flies toward sucrose (Al-Anzi et al., 2006). As a third possibility, we rather believe that expressing the capsaicin receptor in GH86 activates functionally different neurons mediating attractive or aversive stimuli, respectively, which may result in indifferent behavior. Taken together with a previous tetanus toxin expression study (Heimbeck et al., 1999), our data suggest that a subset of GH86-labeled neurons may respond to palatable stimuli like sugars.

The primary larval taste center might thus well be divided into an anterior part, which is labeled by Gr66a-Gal4 and responds to aversive stimuli, and a posterior part, which is represented by a subpopulation of GH86 neurons and responds to attractive cues. This difference, if it in fact exists, remains much more subtle than in the adult system, where sweet and bitter responsive neurons have clearly segregated central projections (Thorne et al., 2004; Wang et al., 2004; Marella et al., 2006).

http://doc.rero.ch

Hints about GR expression

In the transgenic lines used, the expression of Gal4 is controlled by the putative promoter region of *Gr* or *ppk* genes (about 1 kb in length). Conclusions from the reporter patterns about native gene expression must thus be taken with caution. Indeed, a number of observations, such as expression in nonneuronal cells in certain lines, pattern differences between different insertion lines (e.g., in Gr22b or Gr66a), the unexpected expression of Gr68a-Gal4 (a receptor proposed to mediate pheromone perception; Bray and Amrein, [2003]) in VPS neurons, or differences with prior reports (Table 1), introduce doubt whether these lines accurately reflect gene expression. Nevertheless, our data provide good evidence for coexpression of multiple taste receptors per cell (Fig. 4), in contrast to a prior report based on fewer lines (Scott et al., 2001). Interestingly, our results suggest coexpression of Gr66a and Ppk 12 (Fig. 3K), which would fit with observations that bitter responsive cells in the adult also respond to salt at high concentration (Meunier et al., 2003).

The four lines, Gr2a-Gal4, Gr59f-Gal4, Gr21a-Gal4, and Ppk6-Gal4, which were not coexpressed with Gr66a-GFP might thus be expressed in neurons responding to different, but perhaps also repulsive, tastants. In contrast to studies in the adult suggesting that the majority of GRs are coexpressed with Gr66a (Thorne et al., 2004; Wang et al., 2004), we found an overlap of only 60%. This discrepancy may be due to a difference between adult and larval systems; alternatively, the data in the adult were incomplete. Indeed, Gr21a was not taken into account in adult studies because it showed expression in olfactory neurons. Also, possible coexpression of Gr2a-Gal4, Gr59f-Gal4, and Ppk-Gal4 with Gr66a-GFP was not checked.

Second-order neurons

An interesting candidate taste interneuron was revealed by the GH146 enhancer trap line. This neuron arborizes in the SOG and extends a process via the lateral horn in the mushroom body calyx, a brain region involved in larval olfactory learning (Honjo and Furukubo-Tokunaga, 2005). The putative dendritic arborization in the SOG extends bilaterally and is larger than afferent projections. Hence, it may receive inputs from different GRNs, suggesting that it may be broadly tuned. Interneurons that possibly link taste inputs with the mushroom bodies were also described in the honeybee (Schröter and Menzel, 2003). Indeed, modulatory function of taste information in the larval mushroom bodies was proposed (Scherer et al., 2003; Honjo and Furukubo-Tokunaga, 2005; Gerber and Hendel, 2006). Such a function was hypothesized to be mediated by octopaminergic neurons in bees (Hammer and Menzel, 1995) and adult *Drosophila* (Thum et al., submitted; Sinakevitch and Strausfeld, 2006). The presence of neurons linking the SOG with the mushroom body calyx suggests that responses toward taste stimuli may be modulated by experience.

A cluster of 20 putative second-order taste neurons, which express the *hugin* neuropeptide, is presented in the accompanying article (Bader et al., 2007). Interestingly, arborizations of these neurons in the SOG are ipsilateral in *area 2* and bilateral in *area 1*, in each of them covering the entire area. This is consistent with afferent projections, supporting direct connectivity between GRNs and the *hugin* cells. Moreover, it suggests that laterality information encoded by the afferents may be sent to the second-order taste neurons and thus to higher brain centers.

Concluding remarks

Previous studies on insect taste centers focused on adults of the flies *D. melanogaster* (Stocker, 1994; Thorne et al., 2004; Wang et al., 2004), *Phormia regina* (Yetman and Pollack, 1986; Edgecomb and Murdock, 1992), and *Neobellieria bullata* (Mitchell and Itagaki, 1992) and of mosquitoes (Ignell and Hansson, 2005). In all these species, central taste projections were shown to be governed primarily by their organ of origin. However, when tested, sensory receptivity also proved to be crucial: attractive and aversive information being segregated. Similar, albeit limited, information was collected from larvae of *Manduca sexta* (Kent and Hildebrand, 1987) and *D. melanogaster* (Scott et al., 2001). Our detailed description shows that subareas of the larval SOG are associated with different organs, similar to the situation in the adult. In contrast, functional divisions of this neuropile were more difficult to assess. The putative second-order neurons described so far exhibit extensive projections in the SOG and may thus receive inputs from different GRNs. We therefore postulate that gustatory target neurons are more broadly tuned than primary ones, similar to the mammalian system (Smith and St John, 1999; Stapleton et al., 2006). This apparent conservation in taste processing is reminiscent of the similarities between the mammalian and insect olfactory systems. If functional studies confirm our anatomical data, *Drosophila* larvae may become an interesting and powerful model for studying how animals decode gustatory information.

ACKNOWLEDGMENTS

We thank Claire Huguenin for technical support, R. Axel and E. Rueckert for sending flies prior to publication, K. Scott, H. Amrein, and M. Welsh for Gal4 lines, and M. Pankratz as well as anonymous reviewers for comments on the article. We also thank all ImageJ developers.

LITERATURE CITED

Al-Anzi B, Tracey WD Jr, Benzer S. 2006. Response of *Drosophila* to Wasabi is mediated by *painless*, the fly homolog of mammalian TRPA1/ANKTM1. Curr Biol 16:1034–1040.

Bader R, Colomb J, Pankratz B, Schröck A, Stocker RF, Pankratz MJ. 2007. Genetic dissection of neural circuit anatomy underlying feeding behavior in *Drosophila:* distinct classes of *hugin* expressing neurons. J Comp Neurol 502:848–856.

Bray S, Amrein H. 2003. A putative *Drosophila* pheromone receptor expressed in male-specific taste neurons is required for efficient courtship. Neuron 39:1019–1029.

Caicedo A, Roper SD. 2001. Taste receptor cells that discriminate between bitter stimuli. Science 291:1557–1560.

Caterina MJ, Schumacher MA, Tominaga M, Rosen TA, Levine JD, Julius D. 1997. The capsaicin receptor: a heat-activated ion channel in the pain pathway. Nature 389:816–824.

Clyne PJ, Warr CG, Carlson JR. 2000. Candidate taste receptors in *Drosophila*. Science 287:1830–1834.

Dahanukar A, Foster K, van Der Goes Van Naters WM, Carlson JR. 2001. A Gr receptor is required for response to the sugar trehalose in taste neurons of *Drosophila*. Nat Neurosci 4:1182–1186.

Dahanukar A, Hallem EA, Carlson JR. 2005. Insect chemoreception. Curr Opin Neurobiol 15:423–430.

Dambly-Chaudière C, Ghysen A. 1986. The sense organs in the *Drosophila*

http://doc.rero.ch

larva and their relation to the embryonic pattern of sensory neurons. Roux's Arch Dev Biol 195:222–228.

Dambly-Chaudière C, Jamet E, Burri M, Bopp D, Basler K, Hafen E, Dumont N, Spielmann P, Ghysen A, Noll M. 1992. The paired box gene *pox neuro*: a determinant of poly-innervated sense organs in *Drosophila*. Cell 69:159–172.

Dunipace L, Meister S, McNealy C, Amrein H. 2001. Spatially restricted expression of candidate taste receptors in the *Drosophila* gustatory system. Curr Biol 11:822–835.

Edgecomb RS, Murdock LL. 1992. Central projections of axons from taste hairs on the labellum and tarsi of the blowfly, Phormia regina Meigen. J Comp Neurol 315:431–444.

Faucher C, Forstreuter M, Hilker M, de Bruyne M. 2006. Behavioral responses of *Drosophila* to biogenic levels of carbon dioxide depend on life-stage, sex and olfactory context. J Exp Biol 209:2739–2748.

Fishilevich E, Domingos AI, Asahina K, Naef F, Vosshall LB, Louis M. 2005. Chemotaxis behavior mediated by single larval olfactory neurons in *Drosophila*. Curr Biol 15:2086–2096.

Gendre N, Lüer K, Friche S, Grillenzoni N, Ramaekers A, Technau GM, Stocker RF. 2004. Integration of complex larval chemosensory organs into the adult nervous system of *Drosophila*. Development 131:83–92.

Gerber B, Hendel T. 2006. Outcome expectations drive learned behaviour in larval *Drosophila*. Proc Biol Sci 273:2965–2968.

Gerber B, Scherer S, Neuser K, Michels B, Hendel T, Stocker RF, Heisenberg M. 2004. Visual learning in individually assayed *Drosophila* larvae. J Exp Biol 207:179–188.

Glendinning JI, Davis A, Ramaswamy S. 2002. Contribution of different taste cells and signaling pathways to the discrimination of "bitter" taste stimuli by an insect. J Neurosci 22:7281–7287.

Hallem EA, Dahanukar A, Carlson JR. 2006. Insect odor and taste receptors. Annu Rev Entomol 51:113–135.

Hammer M, Menzel R. 1995. Learning and memory in the honeybee. J Neurosci 15:1617–1630.

Heimbeck G, Bugnon V, Gendre N, Häberlin C, Stocker RF. 1999. Smell and taste perception in *Drosophila melanogaster* larva: toxin expression studies in chemosensory neurons. J Neurosci 19:6599–6609.

Heimbeck G, Bugnon V, Gendre N, Keller A, Stocker RF. 2001. A central neural circuit for experience-independent olfactory and courtship behavior in *Drosophila melanogaster*. Proc Natl Acad Sci U S A 98: 15336–15341.

Honjo K, Furukubo-Tokunaga K. 2005. Induction of cAMP response element-binding protein-dependent medium-term memory by appetitive gustatory reinforcement in *Drosophila* larvae. J Neurosci 25:7905–7913.

Ignell R, Hansson BS. 2005. Projection patterns of gustatory neurons in the suboesophageal ganglion and tritocerebrum of mosquitoes. J Comp Neurol 492:214–233.

Inomata N, Goto H, Itoh M, Isono K. 2004. A single-amino-acid change of the gustatory receptor gene, Gr5a, has a major effect on trehalose sensitivity in a natural population of *Drosophila melanogaster*. Genetics 167:1749–1758.

Ishimoto H, Tanimura T. 2004. Molecular neurophysiology of taste in *Drosophila*. Cell Mol Life Sci 61:10–18.

Jefferis GS. 2005. Insect olfaction: a map of smell in the brain. Curr Biol 15:R668–670.

Jones LM, Fontanini A, Katz DB. 2006. Gustatory processing: a dynamic systems approach. Curr Opin Neurobiol 16:420–428.

Keller A, Vosshall LB. 2003. Decoding olfaction in *Drosophila*. Curr Opin Neurobiol 13:103–110.

Kent KS, Hildebrand JG. 1987. Cephalic sensory pathways in the central nervous system of larval *Manduca sexta* (Lepidoptera: Sphingidae). Philos Trans R Soc Lond B Biol Sci 315:1–36.

Lee T, Luo L. 1999. Mosaic analysis with a repressible cell marker for studies of gene function in neuronal morphogenesis. Neuron 22:451–461.

Lemon CH, Smith DV. 2005. Neural representation of bitter taste in the nucleus of the solitary tract. J Neurophysiol 94:3719–3729.

Lemon CH, Smith DV. 2006. Influence of response variability on the coding performance of central gustatory neurons. J Neurosci 26:7433–7443.

Lilly M, Carlson J. 1990. *smellblind*: a gene required for *Drosophila* olfaction. Genetics 124:293–302.

Liu L, Leonard AS, Motto DG, Feller MA, Price MP, Johnson WA, Welsh MJ. 2003a. Contribution of *Drosophila DEG/ENaC* genes to salt taste. Neuron 39:133–146.

Liu L, Yermolaieva O, Johnson WA, Abboud FM, Welsh MJ. 2003b. Identification and function of thermosensory neurons in *Drosophila* larvae. Nat Neurosci 6:267–273.

Marella S, Fischler W, Kong P, Asgarian S, Rueckert E, Scott K. 2006. Imaging taste responses in the fly brain reveals a functional map of taste category and behavior. Neuron 49:285–295.

Melcher C, Pankratz MJ. 2005. Candidate gustatory interneurons modulating feeding behavior in the *Drosophila* brain. PLoS Biol 3:e305.

Meunier N, Marion-Poll F, Rospars JP, Tanimura T. 2003. Peripheral coding of bitter taste in *Drosophila*. J Neurobiol 56:139–152.

Meyerhof W. 2005. Elucidation of mammalian bitter taste. Rev Physiol Biochem Pharmacol 154:37–72.

Mitchell BK, Itagaki H. 1992. Interneurons of the subesophageal ganglion of *Sarcophaga bullata* responding to gustatory and mechanosensory stimuli. J Comp Physiol [A] 171:213–230.

Mitchell BK, Itagaki H, Rivet MP. 1999. Peripheral and central structures involved in insect gustation. Microsc Res Tech 47:401–415.

Miyakawa Y. 1982. Behavioral evidence for the existence of sugar, salt and amino acid taste receptor cells and some of their properties in *Drosophila* larvae. J Insect Physiol 28:405–410.

Moon SJ, Kottgen M, Jiao Y, Xu H, Montell C. 2006. A taste receptor required for the caffeine response in vivo. Curr Biol 16:1812–1817.

Mueller KL, Hoon MA, Erlenbach I, Chandrashekar J, Zuker CS, Ryba NJ. 2005. The receptors and coding logic for bitter taste. Nature 434:225–229.

Murphey RK, Possidente D, Pollack G, Merritt DJ. 1989. Modality-specific axonal projections in the CNS of the flies *Phormia* and *Drosophila*. J Comp Neurol 290:185–200.

Nayak SV, Singh RN. 1985. Primary sensory projections from the labella to the brain of *Drosophila melanogaster* Meigen (Diptera: Drosophilidae). Int J Insect Morphol Embryol 14:115–129.

Oppliger FY, Guerin P, Vlimant M. 2000. Neurophysiological and behavioral evidence for an olfactory function for the dorsal organ and a gustatory one for the terminal organ in *Drosophila melanogaster* larvae. J Insect Physiol 46:135–144.

Python F, Stocker RF. 2002. Adult-like complexity of the larval antennal lobe of *D. melanogaster* despite markedly low numbers of odorant receptor neurons. J Comp Neurol 445:374–387.

Rajashekhar KP, Singh RN. 1994. Neuroarchitecture of the tritocerebrum of *Drosophila melanogaster*. J Comp Neurol 349:633–645.

Ramaekers A, Magnenat E, Marin EC, Gendre N, Jefferis GS, Luo L, Stocker RF. 2005. Glomerular maps without cellular redundancy at successive levels of the *Drosophila* larval olfactory circuit. Curr Biol 15:982–992.

Robertson HM, Warr CG, Carlson JR. 2003. Molecular evolution of the insect chemoreceptor gene superfamily in *Drosophila melanogaster*. Proc Natl Acad Sci U S A 100(Suppl 2):14537–14542.

Rutzler M, Zwiebel LJ. 2005. Molecular biology of insect olfaction: recent progress and conceptual models. J Comp Physiol [A] 191:777–790.

Sato T, Beidler LM. 1997. Broad tuning of rat taste cells for four basic taste stimuli. Chem Senses 22:287–293.

Scherer S, Stocker RF, Gerber B. 2003. Olfactory learning in individually assayed *Drosophila* larvae. Learn Mem 10:217–225.

Schröter U, Menzel R. 2003. A new ascending sensory tract to the calyces of the honeybee mushroom body, the subesophageal-calycal tract. J Comp Neurol 465:168–178.

Scott K. 2004. The sweet and the bitter of mammalian taste. Curr Opin Neurobiol 14:423–427.

Scott K, Brady R Jr, Cravchik A, Morozov P, Rzhetsky A, Zuker C, Axel R. 2001. A chemosensory gene family encoding candidate gustatory and olfactory receptors in *Drosophila*. Cell 104:661–673.

Shanbhag SR, Singh RN. 1992. Functional implications of the projections of neurons from individual labellar sensillum of *Drosophila melanogaster* as revealed by neuronal-marker horseradish peroxidase. Cell Tissue Res 267:273–282.

Sinakevitch I, Strausfeld NJ. 2006. Comparison of octopamine-like immunoreactivity in the brains of the fruit fly and blow fly. J Comp Neurol 494:460–475.

Singh RN, Singh K. 1984. Fine structure of the sensory organs of *Drosophila melanogaster* Meigen larva. Int J Insect Morphol Embryol 13:255–273.

Smith DV, St John SJ. 1999. Neural coding of gustatory information. Curr Opin Neurobiol 9:427–435.

Stapleton JR, Lavine ML, Wolpert RL, Nicolelis MA, Simon SA. 2006.

http://doc.rero.ch

Rapid taste responses in the gustatory cortex during licking. J Neurosci 26:4126–4138.

Stocker RF. 1994. The organization of the chemosensory system in *Drosophila melanogaster*: a review. Cell Tissue Res 275:3–26.

Stocker RF, Schorderet M. 1981. Cobalt filling of sensory projections from internal and external mouthparts in *Drosophila*. Cell Tissue Res 216: 513–523.

Stocker RF, Heimbeck G, Gendre N, de Belle JS. 1997. Neuroblast ablation in *Drosophila* P[GAL4] lines reveals origins of olfactory interneurons. J Neurobiol 32:443–456.

Suh GS, Wong AM, Hergarden AC, Wang JW, Simon AF, Benzer S, Axel R, Anderson DJ. 2004. A single population of olfactory sensory neurons mediates an innate avoidance behaviour in *Drosophila*. Nature 431: 854–859.

Takagawa K, Salvaterra P. 1996. Analysis of choline acetyltransferase protein in temperature sensitive mutant flies using newly generated monoclonal antibody. Neurosci Res 24:237–243.

Thorne N, Chromey C, Bray S, Amrein H. 2004. Taste perception and coding in *Drosophila*. Curr Biol 14:1065–1079.

Tracey WD Jr, Wilson RI, Laurent G, Benzer S. 2003. *painless*, a *Drosophila* gene essential for nociception. Cell 113:261–273.

Ueno K, Ohta M, Morita H, Mikuni Y, Nakajima S, Yamamoto K, Isono K. 2001. Trehalose sensitivity in *Drosophila* correlates with mutations in and expression of the gustatory receptor gene *Gr5a*. Curr Biol 11:1451–1455.

Wang Z, Singhvi A, Kong P, Scott K. 2004. Taste representations in the *Drosophila* brain. Cell 117:981–991.

Whiteland JL, Nicholls SM, Shimeld C, Easty DL, Williams NA, Hill TJ. 1995. Immunohistochemical detection of T-cell subsets and other leukocytes in paraffin-embedded rat and mouse tissues with monoclonal antibodies. J Histochem Cytochem 43:313–320.

Wong AM, Wang JW, Axel R. 2002. Spatial representation of the glomerular map in the *Drosophila* protocerebrum. Cell 109:229–241.

Yetman S, Pollack GS. 1986. Central projections of labellar taste hairs in the blowfly, *Phormia regina* Meigen. Cell Tissue Res 245:555–561.

Zhao GQ, Zhang Y, Hoon MA, Chandrashekar J, Erlenbach I, Ryba NJ, Zuker CS. 2003. The receptors for mammalian sweet and umami taste. Cell 115:255–266.

http://doc.rero.ch

Supplementary Fig.1 Stack of images showing a 360° rotation of a 3D reconstruction of axon terminals labelled by Ppk6-Gal4 (cf. Fig. **2H**). It shows accurately the closeness of VPS and TO neuron projections.